ELSEVIER

Earth and Planetary Science Letters 148 (1997) 471–483

EPSL

Trace element evidence from seamounts for recycled oceanic crust in the Eastern Pacific mantle

Yaoling Niu [a,*], Rodey Batiza [b]

[a] Department of Earth Sciences, The University of Queensland, Brisbane, Qld 4072, Australia
[b] Department of Geology and Geophysics and Hawaii Center for Volcanology, University of Hawaii, Honolulu, HI 96822, USA

Received 11 June 1996; revised 27 January 1997; accepted 25 February 1997

Abstract

We present trace element data for 80 samples from about 50 seamounts in the east equatorial Pacific near the East Pacific Rise. These data indicate that the heterogeneous mantle source that supplies the seamounts consists of two components: (1) an extremely depleted component, much more depleted than estimates of the source of depleted MORB; and (2) an enriched component even more enriched than average OIB. The depleted component shows large variations in Zr/Hf, Nb/Ta, Rb/Cs, Ce/Pb, and Th/U that are correlated with each other and with La/Sm, indicating that these paired elements do fractionate from each other in some oceanic basalts. The order of incompatibility of trace elements we find differs slightly from that found elsewhere. For example, for seamounts, we find that $D_{Nb} \approx D_{Th} < D_{Ta} \approx D_U$. In comparison with Th and U, the enriched component shows anomalous enrichments of Ta and Nb. Since such fractionations are characteristic of subduction zones, we suggest that the most likely ultimate source of the enriched component is recycled ocean crust.

Keywords: seamounts; East Pacific Rise; basalts; trace elements; mantle source heterogeneity; oceanic crust recycling

1. Introduction

Isotopic and trace element studies of oceanic basalts provide fundamental constraints for models of earth's differentiation and convection processes (e.g. [1–7]). It is generally thought that mid-ocean ridge basalts (MORB) are derived from a mantle source that was depleted early in earth history to produce the continental crust. Hofmann and colleagues [3,8] argue that this early differentiation event resulted in a relatively homogeneous mantle, from which the depleted source for MORB and the more enriched source of Ocean Island Basalt (OIB) were then produced over a long period, principally by the subduction of oceanic crust [9].

Data from oceanic basalts have led to the identification of several distinct mantle reservoirs and components [1], whose origin and significance is actively debated [5,10,11]. In addition to lavas from mid-ocean ridges and large hotspot volcanoes, samples from small seamounts near the East Pacific Rise have previously provided useful windows to the suboceanic mantle (e.g. [12–14]). These studies, and others, have shown that near-axis seamounts are geochemically more diverse than basalts erupted at the axis. Despite the greater diversity of seamount lavas, reflecting heterogeneity of the mantle source, the mean composition of seamount lavas is very

* Corresponding author. Tel.: +61 7 3365 2372. Fax: +61 7 3365 1277. E-mail: niu@earthsciences.uq.edu.au

PII S0012-821X(97)00048-4

similar to axial MORB, after considering the fact that seamount lavas are generally more primitive, with higher abundances of MgO [15].

In this paper, we present new trace element data for about 50 near-ridge seamounts near the East Pacific Rise between 5° and 15°N. The samples are a subset of those previously studied [15]. Our results confirm that seamount lavas in this part of the Pacific are extremely heterogeneous but can be readily explained by melting of a mantle source consisting of two components, one enriched in incompatible elements and the other depleted in incompatible elements. The geochemical consequence of melting such a source is to produce the apparent mixing relationships in the melts between the two components

Table 1
Blank levels and USGS reference standards BIR-1 and AGV-1 analyzed by ICP–MS at The University of Queensland

	AGV-1 (ppm)	RSD (%)	BIR-1 (ppm)	RSD (%)	Blank (ppb)	1σ
Li	12.1	5.4	3.11	2.7	0.056	0.040
Be	2.20	4.7	0.091	8.8	0.019	0.028
Sc	12.4	3.4	43.5	1.6	2.071	2.547
V	111	1.8	283	3.5	0.088	0.087
Cr	8.7	5.5	373	3.1	0.755	0.786
Co	16.0	2.7	55	7.1	0.239	0.193
Ni	16.6	4.6	170	2.1	2.156	1.175
Cu	62.5	2.0	121	2.2	0.229	0.100
Zn	81.9	3.0	66	3.9	2.058	0.855
Ga	20.3	2.4	15.4	2.3	0.074	0.094
Rb	66.6	1.8	0.20	4.4	0.044	0.031
Sr	646	1.8	109	1.3	1.240	2.187
Y	17.4	2.1	13.5	2.4	0.003	0.001
Zr	211	1.7	13.1	2.0	0.007	0.003
Nb	14.2	1.6	0.54	1.2	0.008	0.005
Cs	1.26	2.4	0.005	9.9	0.005	0.003
Ba	1162	2.8	6.44	2.1	0.035	0.016
La	37.6	2.2	0.58	3.4	0.004	0.001
Ce	67.2	2.3	1.84	1.7	0.004	0.002
Pr	8.71	2.1	0.38	1.8	0.003	0.001
Nd	30.2	2.5	2.24	1.7	0.007	0.002
Sm	5.44	2.2	1.02	1.5	0.017	0.009
Eu	1.54	5.4	0.49	1.7	0.003	0.001
Gd	5.16	4.1	1.67	3.2	0.011	0.003
Tb	0.61	3.0	0.32	2.6	0.001	0.000
Dy	3.37	2.6	2.38	2.2	0.006	0.002
Ho	0.64	2.4	0.52	2.4	0.002	0.001
Er	1.79	2.3	1.54	2.5	0.004	0.001
Tm	0.23	2.2	0.22	2.1	0.001	0.000
Yb	1.54	1.8	1.49	2.8	0.004	0.001
Lu	0.23	2.6	0.22	2.1	0.001	0.000
Hf	4.91	2.0	0.53	1.8	0.005	0.001
Ta	0.84	2.4	0.049	1.1	0.003	0.001
Pb	32.5	0.8	2.81	3.1	0.015	0.005
Th	5.90	2.1	0.030	6.6	0.002	0.000
U	1.88	1.9	0.011	4.4	0.005	0.011

Notes to Table 1:
We analyzed fresh, hand picked glasses lightly leached in 10% H_2O_2–5% HCl (1:1 by volume), for 10 min to remove any Mn oxides in cracks and other potential labile contaminants, repeatedly washed ultrasonically in mili-Q water, dried, weighed, dissolved. The analyses were done using a Fisons (VG) PQ2 ICP–MS at The University of Queensland. The values for both BIR-1 and AGV-1 are averages of 18 repeated analyses of 12 digestions. The RSD is the relative standard deviation in percent. The blank values are the average of 10 repeated analyses of 6 individual procedural blanks. Note the high 'blank' value (also large σ) for Sr, which is affected by Kr contamination in argon. Sample digestion: (1) 50 mg of cleaned material was digested in a 22 ml Screw-top Savillex® Teflon® beaker using 3 ml HF and 3 ml Aquaregia [3 HCl:1 HNO_3] sealed on a hotplate at ~175°C over night; (2) 2 ml H_2O with 1 ml HNO_3 was added to samples and then the sample was evaporated to incipient dryness; (3) 1 ml HNO_3 was added and again evaporated to incipient dryness (often repeated 2–3 times); (4) after cooling, 1 ml 14 N HNO_3 with 5 ml H_2O was added, with a tight lid was place on it and it was kept on a hotplate at ~110°C over night; and (6) the sample was diluted to a total dissolved solid of ~0.1% with 10 ppb internal standards of ^{115}In, ^{187}Re and ^{205}Tl in a matrix of 2% HNO_3. Calibration was done against multi-element standard solutions made from high purity metals or oxides from Aldrich. Instrumental sensitivity was maintained in the range 20–35 million counts per second for 1 ppm ^{115}In solution (often tuned to higher sensitivity for heavy masses for geochemical purposes). Oxide production was minimized by using a low Ar auxiliary flow rate (~0.5 l/min) and low sample introduction rate (0.5–0.7 ml/min). Molecular (oxides/hydroxides) interferences for REEs are corrected. Drift was minimized by flushing through a rock solution for ~30 min before tuning the instrument for a run. Drift corrections are done, in addition to using the internal standards, by repeatedly analyzing a sample as a drift monitor over the duration of a run. The memory effect was avoided by manual analysis and observing ^{181}Ta count levels between samples in a wash solution of 1% Triton X-100 alternated with 2% HNO_3. All H_2O used was double-distilled mili-Q water, and all acids used were double-distilled, concentrated acids. Solution stability was checked by analyzing diluted samples immediately after dissolution and then again after 10 months. For most elements in most samples, the results are indistinguishable and there are no systematic effects for any elements. All samples were maintained under clean room conditions during the entire procedure. Most samples in Table 2 were analyzed at least three times. A detailed procedure for sample preparation and analysis can be obtained electronically from the authors.

Table 2
Major and trace element analyses of glass samples from near-Ridge seamounts, 5°N–15°N EPR

Sample	R1-14	R1-17	R3-1	R3-3	R3-4	R4-7	R7-13	R8-8	R10-3	R13-1
Lat.	5.77	5.77	5.78	5.78	5.78	5.60	8.14	8.34	8.35	8.40
Long.	102.18	102.18	102.21	102.21	102.21	103.02	103.19	103.06	104.11	104.07
Depth	1834	1834	1773	1773	1773	2263	2020	3180	2741	2140
Electron microprobe analyses (wt. %)										
SiO_2	49.18	49.87	49.12	50.27	50.72	50.65	50.45	50.81	50.29	49.78
TiO_2	1.01	1.20	0.91	1.35	1.92	1.84	1.05	1.51	2.28	2.49
Al_2O_3	16.42	15.38	16.68	15.10	14.89	14.72	14.96	14.18	13.66	17.30
FeOt	8.43	9.42	8.10	9.38	10.35	10.44	9.15	10.97	12.55	8.82
MnO	0.15	0.20	0.15	0.19	0.20	0.21	0.19	0.23	0.23	0.17
MgO	9.35	8.28	9.70	8.26	6.67	6.70	8.47	7.13	6.40	5.87
CaO	12.76	12.69	12.74	12.46	11.25	11.29	13.02	11.92	11.14	9.20
Na_2O	2.29	2.55	2.16	2.52	3.13	3.24	2.24	2.67	2.73	4.01
K_2O	0.04	0.05	0.03	0.06	0.32	0.30	0.05	0.11	0.23	1.36
P_2O_5	0.13	0.15	0.12	0.15	0.23	0.22	0.13	0.16	0.25	0.61
Total	99.75	99.78	99.74	99.75	99.67	99.59	99.71	99.68	99.75	99.63
$Mg^{\#}$	68.73	63.53	70.36	63.56	56.06	55.97	64.70	56.28	50.24	56.87
ICP-MS analyses (ppm)										
Li	4.35	5.40	4.07	4.67	5.12	5.58	4.46	5.31	8.01	6.57
Be	0.26	0.29	0.16	0.19	0.21	0.74	0.17	0.35	0.69	1.81
Sc	33.8	42.9	32.1	35.2	38.9	39.3	38.5	38.7	41.9	24.2
V	196	238	185	203	225	243	226	241	332	194
Cr	326	347	328	377	385	138	346	71.6	108	118
Co	42.7	52.9	42.0	47.5	47.4	38.1	43.8	43.1	45.2	33.2
Ni	87.6	66.0	121	135	95.8	39.5	61.4	29.6	45.5	77.6
Cu	84.7	91.9	77.7	86.1	87.1	84.3	91.1	65.9	79.4	45.7
Zn	55.3	86.2	48.8	65.6	72.7	75.8	57.2	68.1	112	107
Ga	14.0	15.6	13.5	15.2	15.9	16.8	14.5	15.6	19.6	22.0
Rb	0.16	0.37	0.08	0.11	0.14	4.20	0.14	0.70	1.92	26.70
Sr	83.2	90.9	66.3	69.5	69.0	156	57.5	93.7	125	538
Y	20.0	25.4	18.8	19.6	22.0	30.6	21.5	25.6	42.0	27.3
Zr	44.7	64.4	34.5	36.2	40.5	126	37.8	66.8	133	256
Nb	0.525	0.989	0.386	0.394	0.444	7.292	0.581	1.966	4.475	46.001
Cs	0.019	0.022	0.003	0.003	0.004	0.076	0.003	0.010	0.035	0.319
Ba	1.81	2.22	1.27	2.41	1.84	38.32	1.85	9.31	18.91	384.26
La	1.30	1.73	0.92	1.05	1.09	6.77	0.92	2.49	5.41	30.64
Ce	4.64	6.37	3.38	3.69	4.11	18.22	3.55	7.93	16.31	65.15
Pr	0.89	1.17	0.67	0.74	0.83	2.71	0.73	1.37	2.89	8.11
Nd	5.02	6.58	4.04	4.47	4.97	12.87	4.46	7.29	13.84	32.20
Sm	1.90	2.52	1.68	1.83	2.08	3.81	1.86	2.52	4.57	6.69
Eu	0.78	0.99	0.73	0.77	0.85	1.41	0.78	1.00	1.62	2.21
Gd	2.73	3.42	2.49	2.63	2.98	4.76	2.82	3.54	6.11	6.31
Tb	0.49	0.63	0.45	0.49	0.56	0.80	0.52	0.63	1.07	0.91
Dy	3.35	4.18	3.11	3.31	3.73	5.18	3.53	4.21	6.98	5.27
Ho	0.73	0.91	0.68	0.72	0.81	1.10	0.79	0.94	1.55	1.00
Er	2.15	2.57	2.01	2.05	2.30	3.15	2.32	2.71	4.55	2.65
Tm	0.33	0.39	0.30	0.31	0.35	0.47	0.35	0.41	0.62	0.37
Yb	2.06	2.54	1.96	2.05	2.32	3.01	2.25	2.61	4.18	2.43
Lu	0.29	0.37	0.28	0.30	0.34	0.44	0.33	0.38	0.64	0.35
Hf	1.287	1.814	1.121	1.198	1.353	3.014	1.246	1.829	3.451	5.779
Ta	0.049	0.101	0.029	0.038	0.041	0.437	0.046	0.126	0.391	2.599
Pb	0.453	0.457	0.157	0.172	0.222	0.651	0.168	0.347	0.584	2.061
Th	0.046	0.064	0.032	0.027	0.030	0.537	0.046	0.132	0.301	2.938
U	0.024	0.034	0.012	0.015	0.020	0.174	0.016	0.049	0.116	1.023

Sample	R13-2	R15-1	R16-1	R16-2	R17-1	R18-3	R19-4	R20-2	R20-3	R21-6
Lat.	8.40	8.76	8.84	8.84	8.91	8.93	8.94	9.00	9.00	8.89
Long.	104.07	104.54	104.57	104.57	104.57	104.46	104.41	104.37	104.37	104.14
Depth	2140	1682	2985	2985	2715	2720	2267	2837	2837	2657
Electron microprobe analyses (wt. %)										
SiO_2	48.40	48.97	50.39	50.12	50.33	49.99	49.75	51.28	51.81	50.82
TiO_2	1.29	2.38	1.58	1.08	2.23	1.76	1.09	1.50	2.01	1.43
Al_2O_3	17.16	18.10	14.83	16.05	15.08	15.84	16.07	14.73	14.07	15.27
FeOt	8.69	8.89	10.00	8.30	10.11	9.20	8.41	9.86	11.32	9.52
MnO	0.18	0.20	0.23	0.19	0.24	0.19	0.19	0.20	0.21	0.17
MgO	9.17	6.47	7.79	8.63	6.29	7.49	8.64	7.83	6.95	8.31
CaO	11.81	8.95	12.07	12.76	11.12	11.41	12.95	11.42	10.09	11.38
Na_2O	2.78	3.87	2.54	2.41	3.28	3.07	2.47	2.58	2.79	2.52
K_2O	0.14	1.32	0.14	0.08	0.70	0.50	0.08	0.12	0.17	0.12
P_2O_5	0.19	0.57	0.20	0.17	0.35	0.20	0.16	0.18	0.25	0.19
Total	99.80	99.71	99.75	99.79	99.74	99.66	99.81	99.70	99.66	99.72
$Mg^{\#}$	67.64	59.05	60.67	67.32	55.20	61.74	67.03	61.12	54.88	63.36
ICP-MS analyses (ppm)										
Li	4.47	7.29	6.16	4.66	6.74	5.83	4.90	5.65	8.05	5.08
Be	0.55	1.98	0.50	0.37	1.24	0.85	0.37	0.41	0.71	0.40
Sc	31.3	18.0	43.0	36.4	38.0	36.5	37.6	41.8	42.8	37.0
V	185	157	275	216	267	233	212	253	322	239
Cr	448	122	303	305	129	249	336	304	141	295
Co	56.9	33.7	44.9	39.7	39.3	40.5	43.7	45.8	44.5	39.7
Ni	336	114	93.2	76.1	52.4	71.3	99.6	94.4	50.6	79.5
Cu	79.8	43.8	78.1	74.4	81.4	83.2	89.3	76.4	73.6	69.1
Zn	73.8	91.8	87.6	56.9	100	80.7	66.0	79.4	117	66.6
Ga	15.3	22.1	17.3	14.4	20.9	18.2	15.7	16.4	19.9	15.1
Rb	1.35	25.09	1.53	0.86	14.07	8.66	0.32	1.11	2.34	0.87
Sr	204	513	128	120	311	237	126	119	127	110
Y	21.9	26.8	30.8	22.9	32.4	27.1	22.3	27.2	41.6	26.1
Zr	91.5	254	101	69.1	177	129	65.8	88.0	136	77.4
Nb	3.177	43.380	3.298	1.870	23.307	14.002	1.376	2.733	5.019	2.501
Cs	0.017	0.283	0.023	0.021	0.168	0.112	0.006	0.017	0.033	0.019
Ba	15.34	325.52	15.92	9.52	185.19	104.93	4.21	11.59	24.28	9.98
La	4.16	30.04	4.17	2.76	16.73	10.72	2.37	3.29	5.86	3.10
Ce	12.27	65.06	12.69	8.50	38.38	25.21	7.59	10.26	17.26	9.56
Pr	1.89	8.64	2.08	1.43	5.42	3.66	1.39	1.71	2.99	1.60
Nd	9.30	32.19	10.66	7.39	21.93	15.69	7.01	9.06	14.25	8.21
Sm	2.75	6.66	3.46	2.44	5.39	3.99	2.39	2.94	4.59	2.75
Eu	1.10	2.17	1.29	0.97	1.83	1.41	0.93	1.15	1.59	1.05
Gd	3.54	6.39	4.50	3.27	6.03	4.67	3.19	3.97	5.92	3.70
Tb	0.58	0.89	0.79	0.58	0.93	0.74	0.56	0.70	1.03	0.65
Dy	3.72	4.95	5.27	3.84	5.60	4.60	3.70	4.58	6.67	4.38
Ho	0.79	0.99	1.13	0.84	1.17	0.99	0.81	0.97	1.48	0.95
Er	2.22	2.74	3.17	2.43	3.30	2.84	2.41	2.69	4.31	2.79
Tm	0.33	0.35	0.48	0.37	0.44	0.38	0.32	0.41	0.59	0.42
Yb	2.15	2.26	3.16	2.37	2.91	2.50	2.18	2.69	3.94	2.73
Lu	0.32	0.34	0.45	0.34	0.44	0.38	0.33	0.39	0.60	0.39
Hf	2.037	5.255	2.545	1.792	3.907	2.931	1.694	2.285	3.314	2.052
Ta	0.208	2.356	0.214	0.131	1.263	0.764	0.100	0.179	0.303	0.168
Pb	0.502	2.013	0.454	0.390	1.256	0.861	0.360	0.409	0.594	0.502
Th	0.192	2.795	0.214	0.144	1.492	0.953	0.078	0.166	0.319	0.169
U	0.082	0.927	0.084	0.050	0.486	0.305	0.034	0.064	0.114	0.067

Table 2 (continued)

Sample	R22-1	R23-2	R24-1	R24-5	R25-1	R28-3	R28-7	R29-6	R30-30	R31-1	R32-1	R60-1	R61-2	R62-5	R62-7	R63-1	R65-1	R66-1	"R68-5,9"	R69-1
Lat.	8.90	9.03	8.97	8.97	8.88	8.81	8.81	8.70	9.18	9.09	9.09	10.00	10.01	10.03	10.03	10.10	10.13	10.14	10.20	10.33
Long.	104.10	104.05	103.87	103.87	103.79	103.90	103.90	104.08	105.60	105.02	104.92	104.91	104.79	104.19	104.19	103.46	103.41	103.34	103.42	103.64
Depth	2749	3025	3054	3054	1980	1984	1984	2726	1863	2366	3025	2640	2364	2320	2320	2410	2074	2600	3177	2985
Electron microprobe analyses (wt. %)																				
SiO_2	51.92	49.18	51.08	51.68	50.21	50.97	49.85	49.73	48.94	49.99	49.80	47.76	48.48	49.15	49.31	50.22	49.42	49.52	51.94	51.32
TiO_2	1.33	0.98	1.40	2.07	1.26	2.16	1.15	1.44	1.08	1.18	1.47	1.24	1.21	1.17	1.25	1.28	0.99	1.03	3.68	2.94
Al_2O_3	14.67	17.38	14.75	13.97	15.54	13.95	15.94	16.35	16.91	15.74	16.59	17.63	17.55	16.56	16.34	15.22	16.96	16.33	11.70	12.74
FeOt	9.69	8.53	10.07	11.44	8.86	11.55	8.88	8.60	8.35	8.92	8.05	8.34	8.17	8.56	8.63	9.09	8.30	8.57	16.45	14.16
MnO	0.19	0.15	0.21	0.21	0.17	0.22	0.19	0.17	0.17	0.16	0.16	0.16	0.17	0.16	0.16	0.18	0.13	0.17	0.31	0.26
MgO	7.95	9.77	7.68	6.80	8.37	6.78	8.72	8.88	9.29	8.52	8.63	9.62	9.17	8.98	8.89	8.52	8.82	9.18	3.94	5.27
CaO	11.22	11.06	11.52	10.23	12.48	10.83	12.41	11.67	12.03	12.47	11.64	11.87	11.70	12.11	12.08	12.24	12.48	12.27	7.88	9.49
Na_2O	2.45	2.47	2.73	2.81	2.61	2.84	2.41	2.55	2.73	2.42	2.74	2.88	3.09	2.75	2.78	2.74	2.41	2.46	3.07	3.15
K_2O	0.08	0.06	0.07	0.16	0.09	0.16	0.06	0.15	0.04	0.12	0.34	0.09	0.05	0.10	0.11	0.07	0.07	0.07	0.35	0.25
P_2O_5	0.18	0.15	0.16	0.24	0.11	0.24	0.16	0.19	0.15	0.16	0.24	0.13	0.15	0.15	0.15	0.15	0.12	0.14	0.37	0.20
Total	99.69	99.72	99.67	99.61	99.68	99.71	99.76	99.73	99.69	99.68	99.68	99.73	99.74	99.70	99.71	99.71	99.69	99.73	99.68	99.77
$Mg^{\#}$	61.92	69.42	60.18	54.07	65.17	53.76	66.04	67.17	68.79	65.42	67.97	69.54	68.96	67.52	67.11	65.00	67.80	67.95	32.15	42.46
ICP-MS analyses (ppm)																				
Li	6.08	4.70	6.47	6.94	4.52	6.84	5.50	4.69	5.47	4.25	4.96	3.61	4.66	4.62	4.36	5.50	4.04	4.43	13.88	10.07
Be	0.41	0.29	0.42	0.60	0.36	0.59	0.33	0.46	0.26	0.31	0.82	0.39	0.36	0.39	0.38	0.34	0.28	0.25	1.28	0.96
Sc	43.7	33.8	45.0	39.5	37.8	39.3	39.7	32.3	34.8	34.7	34.4	26.8	32.5	37.4	33.5	42.8	32.4	33.4	44.0	44.1
V	271	174	272	302	213	301	234	218	199	206	225	148	184	205	191	233	180	191	470	431
Cr	226	444	217	124	317	130	341	286	320	316	312	380	373	303	279	359	383	309	-	40
Co	45.3	54.8	47.2	38.6	39.6	38.3	47.7	39.7	48.3	40.9	43.1	39.0	49.0	46.0	40.6	45.5	45.3	42.5	51.0	49.7
Ni	53.7	334	57.2	48.1	67.8	48.8	99.6	146	119	97.3	156	222	200	112	93.0	80.2	145	93.9	13.6	29.9
Cu	85.6	107	87.4	62.8	79.0	61.5	93.9	63.6	91.0	79.5	65.3	62.0	83.9	87.2	77.1	89.1	93.4	83.3	79.1	70.9
Zn	83.3	80.4	86.1	86.9	59.5	83.6	73.8	62.1	79.3	54.8	79.8	43.5	71.0	68.2	53.5	84.1	50.5	51.2	189	151
Ga	17.4	15.5	17.9	16.7	14.3	16.4	16.5	15.2	16.2	14.1	17.4	12.1	15.9	16.0	14.4	15.9	13.7	13.8	26.6	23.5
Rb	0.54	0.33	0.26	1.56	0.28	1.59	0.20	1.39	0.42	1.01	7.17	0.46	0.23	1.10	0.81	0.40	0.26	0.25	4.00	2.50
Sr	98.7	103	109	111	116	111	104	120	100	110	219	152	152	149	133	118	101	92.9	128	126
Y	29.9	20.8	30.5	39.5	22.6	39.0	24.6	25.3	21.8	20.8	24.2	17.9	20.8	22.5	21.6	25.2	18.2	20.0	74.2	58.3
Zr	79.7	49.4	81.9	127	67.1	125	62.8	84.7	52.3	58.0	113	66.5	69.6	76.2	67.3	74.2	48.1	47.5	260	194
Nb	1.887	1.069	1.287	3.635	1.212	3.537	0.969	3.580	0.573	1.869	8.879	1.545	0.809	2.683	2.320	1.384	1.012	0.954	8.761	5.869
Cs	0.008	0.006	0.005	0.033	0.006	0.033	0.004	0.021	0.025	0.015	0.122	0.005	0.004	0.020	0.012	0.006	0.005	0.005	0.056	0.037
Ba	6.16	3.12	2.87	15.36	3.62	15.20	2.03	14.83	3.52	10.24	76.18	6.04	2.99	10.69	10.73	2.88	3.05	3.01	34.39	27.12
La	2.77	1.63	2.54	4.90	2.29	4.82	1.98	3.86	1.38	2.43	8.49	2.36	2.04	3.09	2.76	2.36	1.73	1.51	10.06	7.47
Ce	9.01	5.42	8.75	15.21	7.63	14.91	6.77	11.28	5.45	7.36	21.09	7.75	7.65	9.39	8.49	8.07	5.57	5.11	30.94	23.32
Pr	1.68	1.05	1.69	2.52	1.33	2.49	1.31	1.78	1.10	1.21	2.93	1.32	1.44	1.57	1.42	1.44	0.95	0.93	5.18	3.91
Nd	9.35	5.94	8.76	12.84	7.02	12.74	6.88	8.88	6.28	6.26	13.02	6.77	7.70	8.16	7.38	7.76	5.01	5.20	26.33	19.88
Sm	2.98	2.03	3.10	4.30	2.41	4.21	2.50	2.85	2.34	2.10	3.49	2.19	2.53	2.70	2.43	2.70	1.78	1.92	8.43	6.45
Eu	1.12	0.82	1.19	1.49	0.96	1.47	0.98	1.07	0.94	0.87	1.26	0.89	1.00	1.09	0.98	1.09	0.74	0.80	2.67	2.16
Gd	4.11	2.88	4.25	5.62	3.22	5.52	3.48	3.69	3.12	2.96	4.07	2.75	3.13	3.51	3.18	3.72	2.50	2.77	10.45	8.20
Tb	0.74	0.51	0.76	1.00	0.57	0.97	0.62	0.63	0.57	0.51	0.67	0.47	0.56	0.60	0.55	0.65	0.45	0.49	1.86	1.46
Dy	4.81	3.44	4.96	6.60	3.81	6.45	4.09	4.22	3.72	3.46	4.27	3.06	3.62	3.96	3.66	4.28	3.03	3.33	12.27	9.56
Ho	1.08	0.77	1.10	1.44	0.83	1.41	0.91	0.91	0.80	0.76	0.89	0.65	0.77	0.84	0.79	0.91	0.67	0.74	2.63	2.08
Er	3.17	2.28	3.23	4.19	2.41	4.11	2.66	2.62	2.26	2.19	2.50	1.88	2.14	2.31	2.26	2.56	1.97	2.13	7.55	5.92
Tm	0.44	0.31	0.44	0.64	0.36	0.63	0.37	0.39	0.34	0.33	0.37	0.27	0.33	0.34	0.33	0.38	0.29	0.32	1.15	0.91
Yb	2.89	2.08	2.96	4.08	2.32	4.04	2.46	2.59	2.24	2.14	2.43	1.81	2.12	2.25	2.16	2.51	1.94	2.07	7.64	5.97
Lu	0.45	0.32	0.45	0.59	0.33	0.59	0.38	0.37	0.33	0.31	0.35	0.26	0.31	0.33	0.32	0.37	0.28	0.30	1.11	0.87
Hf	2.104	1.396	2.160	3.366	1.770	3.307	1.749	2.162	1.605	1.563	2.647	1.622	1.851	1.933	1.774	1.968	1.312	1.399	6.801	5.059
Ta	0.130	0.081	0.097	0.244	0.089	0.242	0.080	0.226	0.051	0.119	0.539	0.102	0.071	0.171	0.148	0.098	0.069	0.068	0.564	0.391
Pb	0.376	0.247	0.363	0.567	0.377	0.552	0.304	0.503	0.277	0.309	0.781	0.377	0.328	0.347	0.347	0.347	0.284	0.240	0.965	0.777
Th	0.108	0.060	0.070	0.277	0.089	0.270	0.056	0.240	0.042	0.139	0.763	0.102	0.055	0.141	0.152	0.068	0.072	0.071	0.488	0.352
U	0.048	0.027	0.038	0.097	0.037	0.094	0.028	0.081	0.021	0.045	0.245	0.037	0.025	0.063	0.056	0.033	0.028	0.027	0.209	0.146

Table 2 (continued)

Sample	R70-1	R71-21	R72-2	R73-1	R74-6	R75-2	R76-1	R78-6	R79-2	R80-1	R81-1	R82-1	R83-3	R84-3	R86-2	R89SG	R9-1	R91-4	R92-6	R93-7
Lat.	10.29	10.26	10.38	10.38	10.62	10.69	10.65	11.22	11.79	11.80	11.53	11.51	11.24	11.48	11.51	11.52	8.39	11.80	11.94	12.29
Long.	103.63	103.74	103.93	103.92	103.84	103.87	103.24	103.58	103.25	103.25	103.56	103.61	103.59	103.87	103.99	103.88	103.52	103.85	103.89	103.64
Depth	2964	3380	2748	2547	2320	3115	2344	2450	1620	1619	2174	2660	2900	2244	2509	2455	3130	2630	2844	2721
Electron microprobe analyses (wt. %)																				
SiO_2	50.94	50.09	49.14	48.89	50.32	54.89	48.70	50.25	49.60	48.53	50.05	49.30	49.62	49.68	49.62	49.84	50.01	50.01	51.17	49.48
TiO_2	2.44	3.70	1.36	1.47	0.94	2.62	0.92	1.52	1.29	1.68	1.14	1.06	1.96	1.63	1.70	1.84	1.48	1.68	3.67	1.36
Al_2O_3	13.14	12.66	16.84	16.94	15.14	12.81	17.05	17.17	17.24	18.03	15.31	16.07	16.10	15.95	16.03	15.38	15.22	15.24	11.77	16.84
FeOt	12.81	15.37	8.87	8.99	8.81	13.34	8.36	7.99	8.10	7.96	9.02	8.67	9.19	8.75	8.96	9.65	9.60	9.37	16.44	8.29
MnO	0.26	0.25	0.18	0.18	0.19	0.26	0.17	0.16	0.17	0.13	0.19	0.16	0.18	0.18	0.17	0.19	0.19	0.18	0.31	0.17
MgO	6.21	5.05	8.84	8.50	9.31	3.29	9.63	7.66	7.61	8.25	8.70	9.17	8.08	8.14	7.90	7.47	8.11	7.91	4.14	8.63
CaO	10.31	8.67	11.18	11.33	12.83	7.50	12.39	10.48	11.36	11.03	12.78	12.77	10.24	12.02	11.73	11.74	12.41	12.15	8.25	11.77
Na_2O	3.20	3.46	2.92	2.98	2.03	3.97	2.34	3.33	3.20	3.26	2.28	2.32	3.29	3.02	3.13	3.20	2.39	2.85	3.31	2.77
K_2O	0.18	0.24	0.23	0.26	0.03	0.48	0.06	0.80	0.81	0.49	0.06	0.06	0.71	0.18	0.24	0.20	0.11	0.15	0.31	0.21
P_2O_5	0.22	0.27	0.17	0.17	0.13	0.55	0.13	0.30	0.28	0.26	0.13	0.13	0.30	0.17	0.19	0.18	0.17	0.18	0.32	0.19
Total	99.70	99.77	99.73	99.71	99.73	99.71	99.75	99.67	99.66	99.63	99.67	99.72	99.67	99.71	99.67	99.69	99.69	99.73	99.70	99.70
$Mg^{\#}$	49.00	39.42	66.39	65.18	67.67	32.83	69.51	65.50	65.05	67.25	65.65	67.70	63.54	64.82	63.59	60.54	62.59	62.58	33.27	67.33
ICP-MS analyses (ppm)																				
Li	11.20	12.99	4.39	4.41	4.46	14.66	4.23	4.66	4.88	4.74	5.08	4.46	6.43	5.30	5.40	5.32	5.79	5.48	13.48	4.81
Be	0.75	1.28	0.53	0.56	0.13	2.01	0.33	0.88	0.96	0.98	0.30	0.25	1.00	0.63	0.75	0.62	0.43	0.49	1.34	0.75
Sc	42.8	45.7	32.2	31.9	41.5	32.2	35.5	27.6	27.3	27.6	41.0	36.1	31.5	40.0	39.0	37.1	39.7	41.3	42.3	33.6
V	338	456	194	195	225	154	192	168	179	171	239	217	229	229	231	228	253	247	463	207
Cr	94	97	252	262	401	44	344	187	238	178	367	394	326	363	311	211	332	307	46	298
Co	47.6	45.3	41.5	42.3	48.7	29.9	49.8	33.7	38.7	35.8	49.0	49.5	46.8	46.4	44.2	37.5	47.4	44.3	46.9	44.9
Ni	67.6	71.3	133	149	99.1	12.4	168	94.9	96.8	120	82.5	123	221	150	114	69.2	99.1	93.4	15.9	122
Cu	68.2	52.1	69.1	68.9	94.7	36.5	89.6	68.0	79.3	60.8	90.0	95.8	63.9	80.8	81.5	63.9	82.6	86.9	62.2	80.3
Zn	122	169	60.5	60.5	69.9	155	67.9	49.9	68.5	52.2	81.2	73.1	83.1	78.6	94.5	73.7	80.8	82.7	185	74.0
Ga	20.4	24.1	15.3	15.4	14.9	26.7	15.5	14.4	16.2	15.0	16.2	15.4	17.1	17.5	17.8	16.0	16.9	17.2	25.5	16.6
Rb	1.94	1.78	2.87	3.33	0.09	5.89	0.80	17.75	17.14	5.34	0.67	0.50	15.05	1.61	2.18	1.69	0.67	1.32	3.72	2.01
Sr	122	111	179	187	56.1	126	110	262	264	248	93.3	88.6	278	184	210	167	115	150	128	177
Y	44.3	80.0	21.9	21.7	19.4	109.5	19.9	20.2	21.2	24.1	23.7	20.3	30.3	25.7	27.2	28.7	29.1	27.7	77.8	24.7
Zr	142	285	83.0	84.1	30.0	423	51.1	111	110	143	56.1	46.1	156	99.1	116	114	91.9	95.1	279	106
Nb	4.312	5.811	5.173	5.960	0.252	14.527	1.870	29.519	28.126	13.540	1.450	1.161	28.775	3.693	4.928	3.915	2.514	3.420	9.342	5.929
Cs	0.028	0.026	0.040	0.049	0.003	0.082	0.010	0.241	0.215	0.070	0.010	0.007	0.188	0.026	0.034	0.030	0.007	0.016	0.054	0.026
Ba	19.96	16.08	40.74	48.57	1.11	58.36	9.95	216.87	216.17	68.31	9.07	7.18	186.28	20.55	27.63	19.47	5.99	15.24	40.47	25.12
La	9.28	10.22	4.59	5.01	0.77	18.91	2.03	18.19	18.19	10.19	2.02	1.64	17.16	4.68	5.86	4.82	3.29	4.02	11.65	6.16
Ce	17.32	33.25	12.29	13.17	2.91	56.88	6.24	34.93	35.46	25.00	6.61	5.35	36.31	13.81	16.93	14.78	10.66	12.39	35.25	16.15
Pr	2.92	5.64	1.86	1.96	0.59	9.25	1.07	3.92	3.98	3.36	1.18	0.95	4.51	2.21	2.65	2.39	1.81	2.05	5.80	2.32
Nd	14.90	28.91	8.92	9.25	3.57	45.92	5.60	14.60	14.91	14.35	6.45	5.15	18.42	10.74	12.54	12.04	9.53	10.58	29.31	10.74
Sm	4.95	9.39	2.65	2.65	1.59	14.05	2.03	3.14	3.31	3.56	2.39	1.96	4.43	3.32	3.69	3.66	3.15	3.39	9.38	3.14
Eu	1.70	2.80	1.04	1.04	0.67	3.82	0.81	1.11	1.17	1.29	0.93	0.77	1.53	1.25	1.36	1.37	1.19	1.31	2.90	1.15
Gd	6.27	11.90	3.26	3.33	2.39	17.43	2.66	3.47	3.67	3.98	3.22	2.62	5.15	3.96	4.33	4.49	4.30	4.39	11.75	3.73
Tb	1.12	2.10	0.56	0.56	0.46	2.98	0.49	0.55	0.58	0.66	0.59	0.49	0.83	0.69	0.74	0.77	0.75	0.75	2.06	0.65
Dy	7.36	13.68	3.70	3.66	3.25	19.14	3.32	3.47	3.70	4.15	4.03	3.34	5.28	4.44	4.68	4.91	4.89	4.88	13.30	4.21
Ho	1.58	2.97	0.80	0.79	0.71	4.11	0.72	0.74	0.76	0.88	0.86	0.72	1.10	0.93	0.99	1.06	1.04	1.04	2.88	0.90
Er	4.50	8.44	2.31	2.28	2.04	11.74	2.04	2.14	2.15	2.53	2.45	2.05	3.07	2.59	2.76	3.00	2.96	2.89	8.28	2.53
Tm	0.68	1.29	0.35	0.34	0.31	1.76	0.31	0.32	0.31	0.38	0.37	0.32	0.46	0.39	0.41	0.45	0.45	0.43	1.26	0.38
Yb	4.54	8.41	2.22	2.20	2.09	11.44	2.08	2.03	2.09	2.39	2.45	2.11	3.00	2.55	2.67	2.86	2.92	2.76	8.14	2.50
Lu	0.66	1.23	0.33	0.32	0.31	1.67	0.30	0.30	0.31	0.35	0.35	0.30	0.44	0.37	0.39	0.41	0.42	0.41	1.20	0.36
Hf	3.718	7.753	1.969	1.989	1.074	11.607	1.434	2.448	2.550	2.903	1.661	1.379	3.466	2.463	2.803	2.739	2.349	2.411	7.443	2.404
Ta	0.290	0.418	0.298	0.341	0.026	0.917	0.123	1.569	1.600	0.742	0.100	0.080	1.593	0.246	0.323	0.239	0.171	0.226	0.617	0.385
Pb	0.616	1.063	0.540	0.563	0.155	1.306	0.262	1.131	1.114	0.853	0.303	0.264	1.077	0.520	0.653	0.580	0.371	0.433	1.084	0.566
Th	0.266	0.408	0.339	0.389	0.020	1.040	0.105	2.368	2.241	0.799	0.097	0.077	1.897	0.222	0.294	0.238	0.135	0.189	0.586	0.356
U	0.109	0.174	0.119	0.134	0.012	0.408	0.042	0.621	0.656	0.256	0.042	0.029	0.587	0.093	0.133	0.091	0.061	0.082	0.231	0.141

Table 2 (continued)

Sample	R94-2	R96-24	R100-1	R102-1	R103-3	R104-1	R105-5	R106-1	R107-8	R109-5	R110-4	R110-5	R111-3	R111-4	R112-2	R116-1	R118-2	R12-1	R121-3	R123-4
Lat.	12.33	13.07	10.14	13.22	13.84	13.90	14.13	14.12	14.16	14.15	14.14	14.14	14.16	14.16	14.15	14.46	14.68	8.37	14.57	14.80
Long.	103.72	103.45	102.77	102.68	103.80	103.75	103.82	103.85	104.45	104.30	104.36	104.36	104.35	104.35	104.36	104.03	103.80	104.65	104.52	104.51
Depth	2694	2577	1816	2350	2870	1851	2679	2746	2169	2610	2760	2760	2640	2640	2762	2876	2594	2865	2879	2580
Electron microprobe analyses (wt. %)																				
SiO_2	51.00	50.38	50.52	50.52	51.14	50.96	50.52	50.27	50.68	50.56	51.91	48.80	49.98	51.51	51.79	48.56	50.93	48.34	50.84	51.09
TiO_2	1.33	1.38	1.37	1.34	1.41	1.62	1.40	1.86	0.96	1.43	2.32	1.87	2.12	2.26	2.33	1.39	1.77	1.27	1.62	1.57
Al_2O_3	14.52	15.31	15.52	15.77	15.13	15.53	15.23	14.75	15.46	15.90	14.69	16.61	16.07	14.74	14.85	17.11	14.93	17.18	14.46	14.89
FeOt	10.20	8.94	8.91	8.95	9.02	9.05	9.00	10.85	8.03	8.34	10.36	9.33	9.30	10.16	10.48	8.95	9.55	8.74	10.22	9.60
MnO	0.19	0.16	0.14	0.17	0.18	0.18	0.17	0.21	0.15	0.17	0.20	0.17	0.18	0.20	0.20	0.17	0.19	0.18	0.21	0.17
MgO	7.59	8.10	7.98	8.04	7.74	7.27	8.34	7.48	8.99	7.79	5.75	8.15	7.37	6.06	5.54	9.02	7.18	9.16	7.49	7.43
CaO	12.05	12.36	12.12	11.97	11.83	11.47	12.00	11.38	12.75	12.10	9.93	11.16	10.70	10.42	10.01	11.09	11.48	11.85	12.09	11.68
Na_2O	2.55	2.75	2.87	2.71	3.03	3.34	2.77	2.65	2.50	2.66	3.64	3.04	3.24	3.54	3.64	3.25	3.34	2.77	2.56	2.95
K_2O	0.10	0.12	0.12	0.11	0.07	0.11	0.08	0.11	0.05	0.48	0.52	0.34	0.46	0.50	0.53	0.05	0.17	0.13	0.09	0.16
P_2O_5	0.14	0.17	0.15	0.14	0.15	0.18	0.16	0.17	0.14	0.23	0.33	0.23	0.28	0.30	0.30	0.13	0.20	0.19	0.15	0.17
Total	99.68	99.67	99.72	99.72	99.71	99.69	99.68	99.73	99.70	99.64	99.65	99.69	99.69	99.68	99.67	99.72	99.72	99.81	99.72	99.72
$Mg^{\#}$	59.60	64.21	63.93	64.02	62.96	61.40	64.74	57.72	68.93	64.92	52.35	63.37	61.07	54.15	51.17	66.61	59.82	67.50	59.20	60.51
ICP-MS analyses (ppm)																				
Li	6.15	4.56	5.17	4.36	6.00	6.07	6.45	7.41	5.14	5.40	5.95	6.56	6.66	6.61	6.52	5.08	6.81	4.45	6.69	6.42
Be	0.35	0.43	0.50	0.43	0.47	0.75	0.52	0.53	0.25	0.75	1.19	0.87	1.18	1.25	1.30	0.58	0.94	0.62	0.43	0.43
Sc	43.7	37.0	42.7	33.7	41.9	41.9	39.4	41.5	36.9	34.2	36.4	34.4	33.7	37.6	38.0	33.9	39.6	33.1	43.4	41.7
V	273	212	232	207	239	230	252	300	209	226	289	243	269	282	303	182	261	187	278	263
Cr	84	267	285	665	227	240	342	254	364	263	38	243	203	229	63	314	131	314	215	225
Co	50.9	37.7	43.6	52.7	43.4	40.0	45.6	45.5	43.8	41.2	32.6	44.3	37.9	39.4	36.2	49.7	40.4	48.9	44.5	43.6
Ni	50.4	73.9	84.8	632	78.9	57.2	113	91.7	107	118	21.7	146	101	101	30.6	224	49.1	218	57.6	72.7
Cu	81.6	68.0	81.8	81.2	78.1	85.8	81.0	70.2	88.0	71.7	48.1	65.2	58.7	57.7	62.0	83.4	78.2	76.4	74.5	81.9
Zn	85.1	59.6	71.0	68.4	75.5	85.2	85.2	102.5	66.0	75.3	88.7	89.0	90.9	96.4	103	70.6	85.5	67.9	88.0	89.6
Ga	17.0	14.4	16.2	15.0	16.5	16.4	17.4	18.3	15.2	17.0	18.4	18.2	20.1	20.2	20.7	16.5	18.5	16.3	17.2	17.1
Rb	1.64	1.24	1.36	0.98	0.47	1.24	0.61	1.22	0.29	8.62	9.09	7.58	6.94	6.87	9.06	0.38	1.71	1.34	0.75	0.62
Sr	104	125	158	126	132	184	111	96.0	86.1	230	176	225	229	232	187	183	174	206	97.9	103
Y	27.3	23.8	25.8	22.3	29.5	30.6	31.0	37.9	22.4	23.3	40.7	32.4	36.4	36.6	41.8	26.8	34.9	23.4	33.2	30.8
Zr	74.8	78.4	94.2	71.4	93.8	136	95.5	118	50.8	100	194	150	176	176	201	100	151	93.9	95.7	84.7
Nb	3.579	3.085	3.345	2.475	1.543	2.725	2.002	3.233	0.816	14.878	16.181	13.728	14.138	13.595	17.274	1.377	4.991	3.344	2.198	1.724
Cs	0.024	0.017	0.029	0.011	0.018	0.078	0.013	0.022	0.008	0.096	0.127	0.083	0.082	0.082	0.107	0.006	0.023	0.018	0.010	0.011
Ba	20.49	16.48	16.46	11.85	5.03	7.62	6.15	11.36	3.34	108.60	100.47	104.17	87.48	89.94	100.36	4.54	18.78	16.42	6.83	6.22
La	3.16	3.44	3.74	2.75	2.96	5.01	3.19	4.23	1.47	10.04	13.09	10.56	11.91	12.04	13.40	3.33	6.71	4.27	3.31	2.80
Ce	9.03	10.24	11.57	8.46	10.22	15.94	10.61	13.43	5.37	22.29	32.11	26.01	29.79	30.50	33.05	11.48	19.70	12.35	10.72	9.28
Pr	1.45	1.66	1.91	1.40	1.89	2.59	1.92	2.27	1.10	3.13	4.47	3.61	4.46	4.26	4.94	2.13	3.23	2.07	1.86	1.77
Nd	7.67	8.44	9.68	7.24	9.89	12.60	9.90	11.98	5.88	12.57	19.83	16.22	18.71	19.02	20.91	10.47	15.60	9.42	10.04	9.30
Sm	2.73	2.71	3.10	2.45	3.34	3.74	3.39	4.09	2.20	3.19	5.33	4.39	5.01	5.14	5.65	3.25	4.27	2.86	3.52	3.18
Eu	1.10	1.05	1.20	0.96	1.28	1.40	1.24	1.46	0.89	1.16	1.79	1.54	1.71	1.74	1.88	1.24	1.51	1.11	1.28	1.17
Gd	3.83	3.53	3.86	3.22	4.36	4.66	4.39	5.38	3.11	3.81	6.28	5.25	5.92	5.96	6.73	4.05	5.31	3.61	4.64	4.31
Tb	0.68	0.61	0.69	0.58	0.77	0.81	0.79	0.96	0.56	0.62	1.05	0.86	0.97	0.98	1.11	0.69	0.90	0.61	0.83	0.76
Dy	4.55	4.03	4.41	3.79	5.04	5.22	5.14	6.46	3.68	3.90	6.84	5.55	6.06	6.25	6.95	4.48	5.73	3.95	5.66	4.99
Ho	1.01	0.88	0.93	0.83	1.09	1.11	1.13	1.40	0.83	0.84	1.48	1.18	1.31	1.33	1.50	0.98	1.26	0.88	1.23	1.10
Er	2.84	2.55	2.59	2.41	3.08	3.09	3.24	3.94	2.42	2.44	4.26	3.32	3.79	3.77	4.38	2.86	3.70	2.51	3.43	3.25
Tm	0.43	0.38	0.39	0.35	0.44	0.47	0.47	0.59	0.34	0.33	0.65	0.50	0.52	0.56	0.60	0.39	0.51	0.35	0.51	0.45
Yb	2.78	2.44	2.53	2.29	2.92	3.03	3.10	3.89	2.23	2.23	4.09	3.19	3.46	3.72	4.00	2.62	3.34	2.30	3.38	2.98
Lu	0.41	0.36	0.37	0.33	0.44	0.44	0.46	0.57	0.34	0.34	0.59	0.46	0.52	0.53	0.61	0.40	0.51	0.35	0.50	0.45
Hf	1.973	2.014	2.315	1.756	2.432	3.078	2.457	3.062	1.475	2.281	4.496	3.379	3.827	3.998	4.468	2.324	3.209	2.109	2.539	2.213
Ta	0.212	0.186	0.223	0.150	0.120	0.208	0.157	0.216	0.065	0.814	0.974	0.759	0.807	0.823	0.982	0.107	0.316	0.218	0.147	0.125
Pb	0.732	0.480	0.462	0.469	0.445	0.835	0.508	0.492	0.295	0.798	1.341	0.895	1.146	1.077	1.270	0.605	0.813	0.488	0.415	0.407
Th	0.256	0.207	0.200	0.136	0.100	0.169	0.127	0.208	0.055	1.044	1.299	0.952	0.939	0.979	1.227	0.092	0.308	0.207	0.129	0.108
U	0.076	0.072	0.087	0.052	0.046	0.099	0.056	0.087	0.021	0.318	0.436	0.298	0.315	0.339	0.441	0.034	0.117	0.080	0.057	0.047

Sample locations are Lat. (latitude) in degrees north; long. (longitude) in degrees west; and depth in meters below sea level. Major element analyses were done using the electron microprobe at the University of Hawaii (analyst: Y. Niu); all these data were normalized to a Smithsonian MORB glass reference standard VG-2, whose working values (SiO_2, 50.57 wt%; TiO_2, 1.85%; Al_2O_3, 14.06%; FeOt, 11.59%; MnO, 0.22%; CaO, 11.12%; Na_2O, 2.63%; K_2O, 0.19%; and P_2O_5, 0.20%) were agreed upon by Jill Karsten, Emily Klein, and Yaoling Niu in 1993. FeOt is total Fe expressed as Fe^{2+}. $Mg^{\#} = Mg/[Mg + Fe^{2+}] \times 100$ with 10% total Fe as Fe^{3+}. Trace element analyses were done using a PQ2 Inductively-coupled Mass Spectrometer at The University of Queensland (analyst: Y. Niu). The samples are fresh glass chips of 0.5–1.0 mm size hand picked under a binocular microscope. See the notes to Table 1 for sample preparation procedures and run conditions.

[12,16–18], which may be termed melting-induced mixing [18]. We place constraints on the nature of the two components: (1) an extremely depleted component, exhibiting highly variable but correlated differences in Zr/Hf, Nb/Ta, Th/U, Rb/Cs and other ratios that generally show little variation between

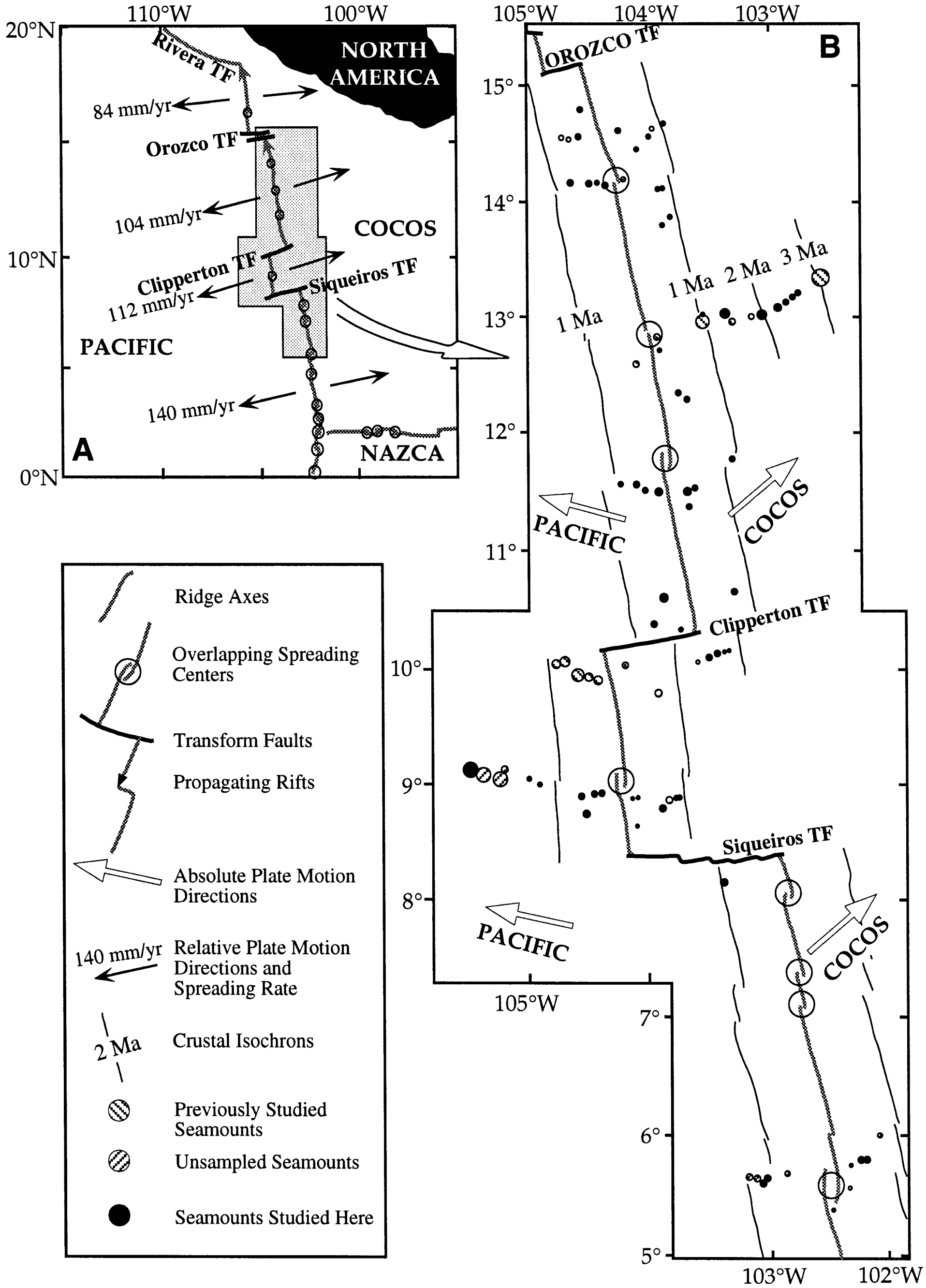

Fig. 1. Location maps for the seamount samples analyzed in this study.

MORB and OIB; and (2) an enriched component with relative enrichments of high-field strength elements (HFSE), such as Nb, Ta, Zr, and Ti. We argue that the enriched component is derived from subducted and recycled oceanic crust [6]. Cousens [19] has recently made a similar proposal to explain the enriched component present in the mantle below the northeast Pacific. Our data show that, at least in this part of the Pacific mantle, even the most depleted seamount and EPR MORB samples are affected by this enrichment process because the depleted end-member is much more depleted than any available lava samples.

2. Data and methods

We analyzed 80 seamount basalt glasses, rock standards, and blanks for trace elements by ICP–MS. Table 1 gives data for the standards and blanks and describes our sample preparation and analytical procedures. Table 2 gives major and trace element analyses of our samples. Major elements were determined on fresh glasses by electron microprobe [15] and trace elements were determined by ICP–MS at the University of Queensland.

3. Results

Fig. 1 shows sample locations and Fig. 2 shows a plot of the trace element data normalized to primitive mantle [3,5]. Also shown are estimates of average continental crust [20], OIB, and both normal (N-type) and enriched (E-type) MORB [5]. The samples exhibit a huge range of variation, from OIB-like lavas to extremely depleted samples. The depleted samples are similar to the most depleted MORB recovered from the EPR (e.g. [21]) and are more depleted than samples from the Lamont Seamounts near 10°N [14].

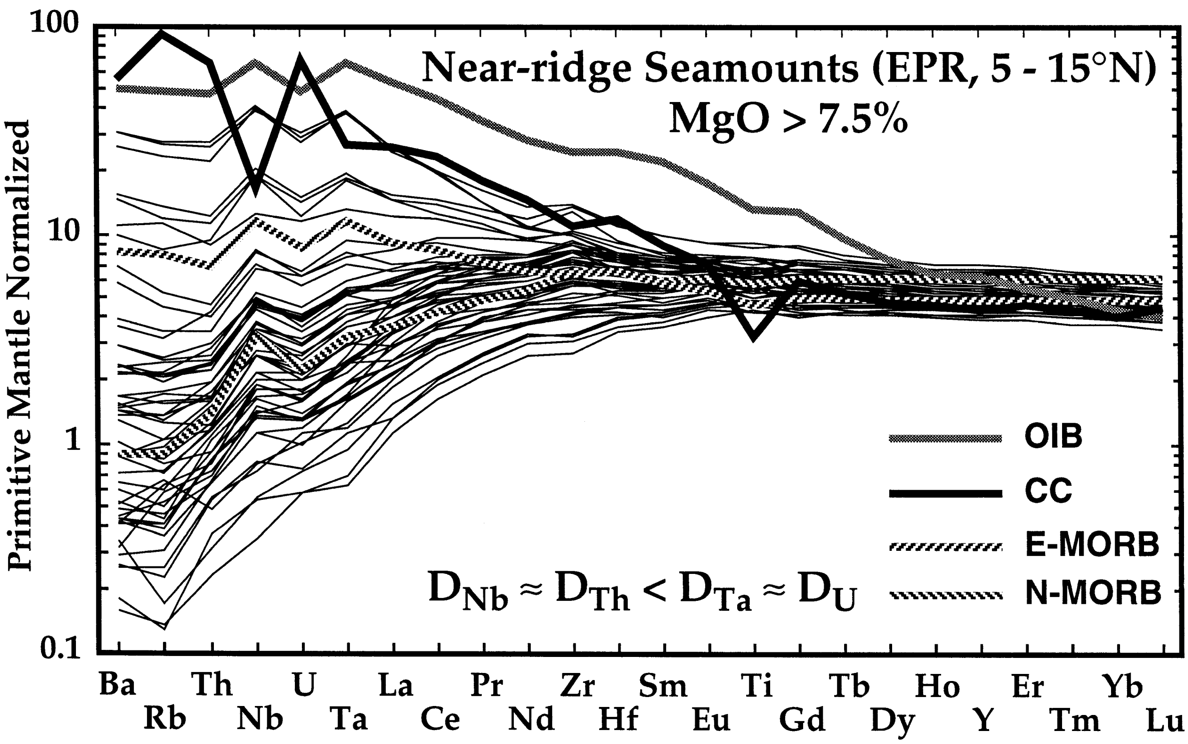

Fig. 2. Primitive mantle-normalized trace element abundances of seamount samples. Also shown are Ocean Island Basalt (OIB), E-MORB and N-MORB [5] and average continental crust [20]. Note that the Nb and Ta depletion of continental crust is matched by enrichments of oceanic basalts. For the seamount samples, enrichments of Nb and Ta increase with increasing overall enrichment.

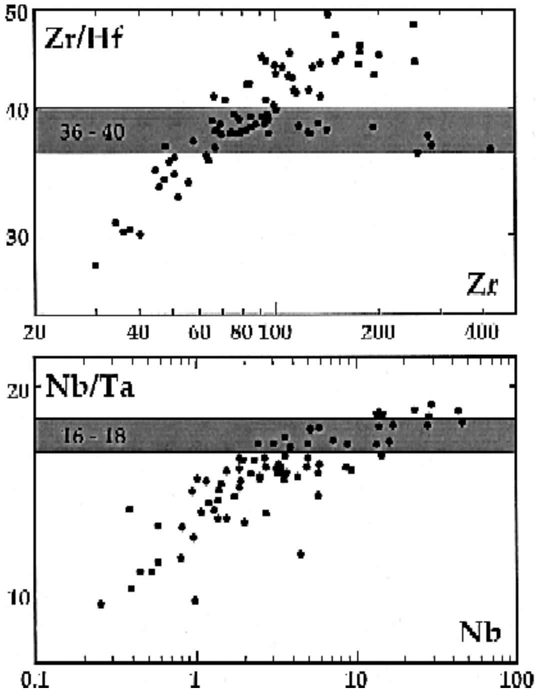

Fig. 3. Plots of Zr/Hf vs. Zr and Nb/Ta vs. Nb for the seamount data. Note that these data indicate that $D_{Zr} < D_{Hf}$ and $D_{Nb} < D_{Ta}$. Similar plots were used to determine the order of incompatibility shown in Fig. 2. Note the wide variation of element ratios, these generally show very limited variation (shaded band) in oceanic basalts.

As found previously, both enriched and depleted samples may occur on the same seamount and we find no systematics to the geographic distribution of enriched and depleted samples. Enriched samples occur on seamounts as close as 4 km from the axis of the EPR.

The order of incompatibility shown in Fig. 2 differs slightly from the order conventionally used by others [3,5]. To determine the order, we used ratio-element plots of the type shown in Fig. 3. Plots such as these can confidently be used to infer which element of the plotted pair is more incompatible [8,22]. The fact that we find a slightly different order of incompatibility is perhaps not surprising, because

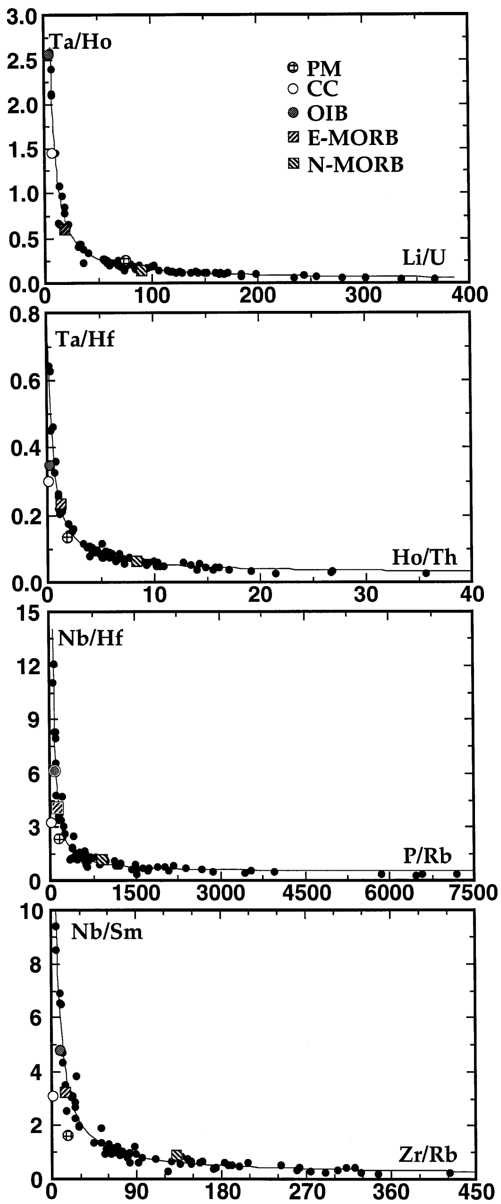

Fig. 4. Plots of various highly and moderately incompatible element pairs (Ta/Ho vs. Li/U; Ta/Hf vs. Ho/Th; Nb/Hf vs. P/Pr; Nb/Sm vs. Zr/Rb) to show that the seamount lavas can be explained by melting-induced two-component mixing; that is, the consequence of melting a two-component mantle source [12,13,16–18]. Note that the hyperbolae are not synonymous with binary mixing of two singular melts [23,24], since the seamounts are geographically dispersed. These hyperbolic plots constrain the nature of the mixing end-members. The depleted end-member is more depleted than previously proposed compositions of depleted MORB mantle. The enriched end-member cannot be average continental crust. We suggest that it is recycled ocean crust with a prior history of subduction-related melting [6].

this order is expected to vary with tectonic setting, differences in mantle sources and differences in the melting process [5]. The most significant differences we find in the order of incompatibility are in the relative incompatibility of Nb, Th, Ta, and U. We find that, in this part of the Pacific mantle, $D_{Nb} \approx D_{Th} < D_{Ta} \approx D_U$. Note that the patterns in Fig. 2 are quite smooth, showing that the order of incompatibility that we use is indeed appropriate for this sample set.

As shown in Fig. 4, the trace element variations are apparently the result of melting-induced two-component mixing. We have made plots using dozens of different ratios and all are consistent with such two-component mixing. The mixing curves can be linear or hyperbolic [23,24] on ratio–ratio diagrams, depending on the differences in relative incompatibility between the two elements in the numerator and in the denominator. The hyperbolic plots, however, constrain the nature of the mixing end-members. The depleted component is extremely depleted. A conservative estimate gives: Zr/Hf $\leq$ 25, Nb/Ta $\leq$ 10, Th/U $\leq$ 1.5, Nb/U $\leq$ 20, Rb/Cs $\leq$ 20 and Ce/Pb $\leq$ 15. On the other hand, the enriched end-member is more enriched that average OIB and resembles average continental crust (CC) in many ways. However, it is clear from Fig. 4 and other plots involving Ta and Nb, that CC can not be the enriched end-member, being far too depleted in these elements.

Fig. 2 shows that the negative anomalies of Ta, Nb, Zr and other HFSE seen in CC are matched by positive anomalies in our samples. This is especially clear for Ta and Nb. Further, the positive anomalies grow larger with progressive enrichment. This is also shown in Fig. 5, indicating qualitatively that the Ta and Nb missing from continental crust may reside in the mantle source of oceanic basalts [4–6], particularly in an enriched component.

As shown in Fig. 3, our samples show relatively large variations in Zr/Hf (28–49). This is also true for Nb/Ta (10–18), Rb/Cs (8–98), Ce/Pb (10–44), Th/U (1.4–3.8) and other element ratios (Fig. 6) that are generally constant for oceanic basalts [8,22,25–28]. Variations of this type were found previously in intraplate basaltic rocks [29]. Further, variations in these ratios show good correlations with each other (R = 0.7–0.8) and with La/Sm. This finding indicates that these element pairs have fractionated from each other, either during formation or modification of the depleted mantle source, or during melting to produce seamount magmas.

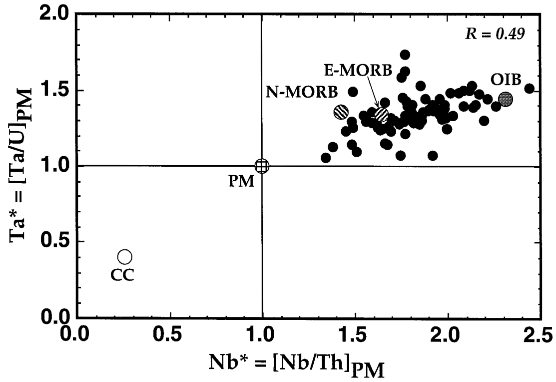

Fig. 5. Excess Ta (Ta^* = [Ta/U] normalized to primitive mantle) plotted against excess Nb for our samples. Note that all our samples, as well as average oceanic basalts, have excesses of both Ta and Nb relative to primitive mantle, while continental crust shows a depletion. We propose that the excess Nb and Ta results from the incorporation of low degree melts into the highly depleted source of N-MORB. Further, we suggest that the ultimate source of these melts is recycled ocean crust [6,9] with a previous history of melting in subduction zones.

To gain insight into the nature of this process, we plot the variability of each element for seamount and EPR axis basalts. Fig. 7 shows that the relative variability of the elements varies rather smoothly with their order of incompatibility, as previously found for other suites [8,30]. Furthermore, the patterns are the same for seamount and axial lavas. This observation provides strong evidence that the process leading to the observed correlated fractionations in Zr/Hf, Nb/Ta, Rb/Cs, Ce/Pb, Th/U, La/Sm and other ratios is a melting process [30]. Additional evidence for this comes from a plot of our data similar to Fig. 2, but with the data normalized to the most depleted seamount sample. This plot (not shown) indicates very smooth and regular increases in incompatible element abundances in progressively enriched samples.

4. Discussion and conclusions

The data presented above shows that the mantle sampled by near-EPR seamounts in the east Equato-

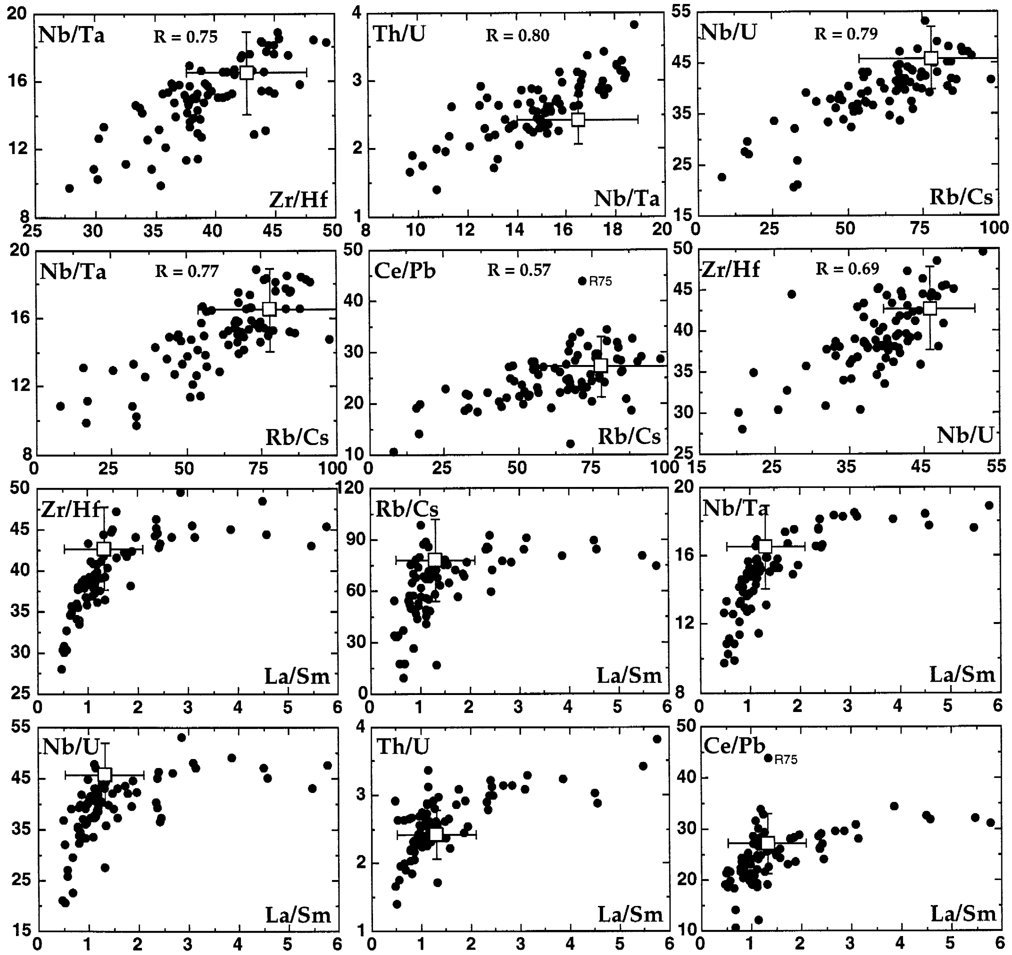

Fig. 6. Trace element ratio–ratio plots of seamount data to show correlations. Note that the plots involving La/Sm (bottom set of panels) show curved data arrays. Also shown (square) is the mean of axial EPR data from 5° to 15°N, with 4σ bars. R75, labeled on plots involving Ce/Pb, is a basaltic andesite with 54 wt% SiO_2.

rial Pacific consists of two end-members: an extremely depleted one, much more depleted than estimates of the depleted MORB mantle [1,2,5,7], and a highly enriched component derived from a source with anomalous enrichments of Nb and Ta relative to Th and U. These end-members are mixed in various proportions prior to or during melting to produce seamount magmas. Physically, these heterogeneous mantle domains must be rather small, perhaps on the order of several hundred meters, in order to explain the great diversity seen in the lavas of single seamounts. It seems reasonable that the enriched component represents highly localized dikes or veins, as previously proposed (e.g. [11,13,16,31]).

Important clues about the origin of the enriched component are its enriched nature and its enrichments of Nb and Ta relative to Th and U. It is widely believed that fractionation of Nb and Ta from Th and U occurs only in subduction zones, although the mechanism is controversial [6,32–34]. There appears to be wide agreement that, whatever the reason for the relative HFSE-depletion of arc magmas, it is likely that there is a complementary enrichment in other reservoirs, such as subducted hydrous ocean

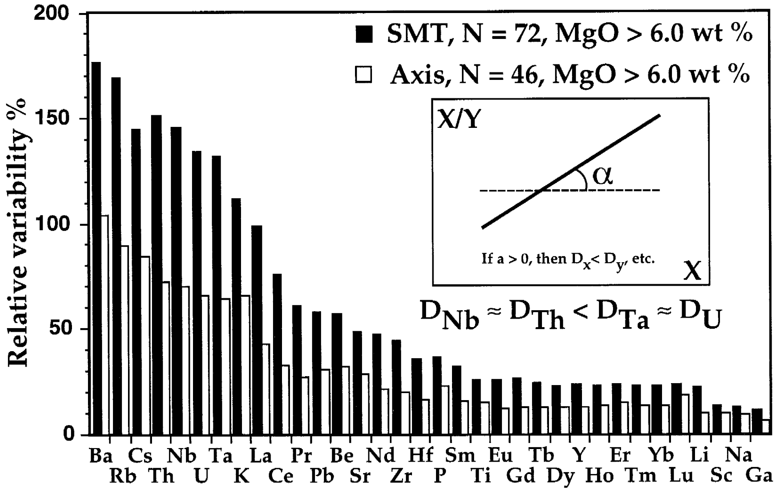

Fig. 7. Relative variability of trace element abundances in seamount samples (this study) and nearby axial samples from the East Pacific Rise (Niu and Batiza, unpubl. data for EPR samples from 9–10°N, 11°20′N, and 13–14°N) plotted against their order of incompatibility, as in [8,30] (Fig. 2). Relative variability is essentially a measure of the mixing contribution from the enriched and depleted end-members. Note the smooth variation for seamount samples and the similar trend shown by the axial samples. We interpret this smooth variation as indicating that element fractionations such as those seen in Fig. 5 are the result of a magmatic (melting) process.

crust [6] and perhaps the mantle portion of the slab, or else the mantle wedge [33]. We propose that the overall enrichment of the enriched seamount component, as well as its relative enrichment of Nb and Ta, point to subducted oceanic crust as a likely candidate for this component.

If so, then one possibility is that this enriched material has simply been mixed into the upper mantle below the east Equatorial Pacific by convective processes (e.g. [35]). Once mixed with depleted mantle, upwelling could cause small amounts of melting and these melts could be dispersed as highly mobile, metasomatic fluids (e.g. [18]), possibly in the low-velocity asthenosphere [36]. We favor this scenario because recent mantle convection models favor only episodic mixing between the upper and lower mantle (e.g. [37]) and because the apparent absence of other enriched components in the east Equatorial Pacific does not suggest a well-stirred, multi-component blend [7]. In addition, the small size scale of the heterogeneities and the absence of larger-scale geographic gradients in trace element abundances in the area both suggest wide, but 'spotty' dispersal, consistent with a metasomatic or low-degree melt origin.

In conclusion, the new trace element data we present provide strong evidence for the involvement of recycled ocean crust in the east Equatorial Pacific mantle source of seamount lavas. These data also provide additional evidence [6] that the missing Nb and Ta in continental crust reside in the mantle source of oceanic basalts.

Acknowledgements

We thank Al Hofmann, Andy Saunders, Francis Albarède, and an anonymous reviewers for constructive comments. Supports by the US NSF and ONR, the Australian ARC, and The University of Queensland are gratefully Acknowledged. This is SOEST Contribution Number 4462. ***[FA]***

References

[1] A. Zindler, S. Hart, Chemical geodynamics, Annu. Rev. Earth Planet. Sci. 14 (1986) 493–571.

[2] C.J. Allègre, Isotope geodynamics, Earth Planet. Sci. Lett. 86 (1987) 175–203.

[3] A.W. Hofmann, Chemical differentiation of the Earth: the relationship between mantle, continental crust, and oceanic crust, Earth Planet. Sci. Lett. 90 (1988) 297–314.

[4] A.D. Saunders, M.J. Norry, J. Tarney, Origin of MORB and chemically-depleted mantle reservoirs: trace element constraints, J. Petrol. Spec. Lithosphere Issue (1988) 415–445.

[5] S.-s. Sun, W.F. McDonough, Chemical and isotopic system-

atics of oceanic basalts: implications for mantle composition and processes, in: A.D. Saunders, M.J. Norry (Eds.), Magmatism in the Ocean Basins, Geol. Soc. London Spec. Publ. 2 (1989) 313–345.
[6] W.F. McDonough, Partial melting of subducted oceanic crust and isolation of its residual eclogitic lithology, Philos. Trans. R. Soc. London Ser. A 335 (1991) 407–418.
[7] S. Hart, A. Zindler, Constraints on the nature and development of chemical heterogeneities in the mantle, in: W.R. Peltier (Ed.), Mantle Convection, Gordon and Breach, 1989, pp. 262–387.
[8] A.W. Hofmann, K.P. Jochum, M. Seufert, W.M. White, Nb and Pb in oceanic basalts: new constraints on mantle evolution, Earth Planet. Sci. Lett. 79 (1986) 33–45.
[9] A.W. Hofmann, W.M. White, Mantle plumes from ancient oceanic crust, Earth Planet. Sci. Lett. 57 (1982) 421–436.
[10] B.L. Weaver, The origin of ocean island basalt end-member compositions: trace element and isotopic constraints, Earth Planet. Sci. Lett. 104 (1991) 381–397.
[11] C.J. Allègre, P. Schiano, E. Lewin, Differences between oceanic basalts by multitrace element ratio topology, Earth Planet. Sci. Lett. 129 (1995) 1–12.
[12] R. Batiza, D. Vanko, Petrology of Pacific seamounts, J. Geophys. Res. 89 (1984) 11235–11260.
[13] A. Zindler, H. Staudigel, R. Batiza, Isotope and trace element geochemistry of young Pacific seamounts: implications for the scale of mantle heterogeneity, Earth Planet. Sci. Lett. 70 (1984) 175–195.
[14] D.J. Fornari, M.R. Perfit, J.F. Allan, R. Batiza, R. Haymon, A. Barone, W.B.F. Ryan, T. Smith, T. Simkin, Seamounts as windows into mantle processes: Structural and geochemical studies of the Lamont seamounts, Earth Planet. Sci. Lett. 89 (1988) 63–83.
[15] R. Batiza, Y. Niu, W.C. Zayac, Chemistry of seamounts near the East-Pacific Rise: Implications for the geometry of subaxial mantle flow, Geology 18 (1990) 1122–1125.
[16] D.A. Wood, A variably veined suboceanic mantle—genetic significance for mid-ocean ridge basalts from geochemical evidence, Geology 7 (1979) 499–503.
[17] A. Prinzhofer, E. Lewin, C.J. Allègre, Stochastic melting of the marble cake mantle: evidence from local study of the East Pacific Rise at 12°50′N, Earth Planet. Sci. Lett. 92 (1989) 189–206.
[18] Y. Niu, D.G. Waggoner, J.M. Sinton, J.J. Mahoney, Mantle source heterogeneity and melting processes beneath seafloor spreading centers: the East Pacific Rise, 18°–19° S, J. Geophys. Res. 101 (1996) 27711–27733.
[19] B.L. Cousens, Depleted and enriched upper mantle sources for basaltic rocks from diverse tectonic environments in the northeast Pacific ocean: the generation of oceanic alkaline vs. tholeiitic basalts, in: A. Basu, S. Hart (Eds.), Earth Processes, Reading the Isotopic Code, Am. Geophys. Union Geophys. Monogr. 95 (1996) 207–231.
[20] R.L. Rudnick, D.M. Fountain, Nature and composition of the continental crust: a lower crustal perspective, Rev. Geophys. 33 (1995) 267–309.
[21] R. Hékinian, D. Bideau, R. Hébert, Y. Niu, Magmatism in the Garrett transform fault (East Pacific Rise near 13°27′S), J. Geophys. Res. 100 (1995) 10163–10185.
[22] A.W. Hofmann, W.M. White, Ba, Rb, and Cs in the Earth's mantle, Z. Naturforsch 38 (a) (1983) 256–266.
[23] R. Vollmer, Rb–Sr and U–Th–Pb systematics of alkaline rocks: the alkaline rocks from Italy, Geochim. Cosmochim. Acta 40 (1976) 283–295.
[24] C.H. Langmuir, R.D. Vocke, G.N. Hanson, A general mixing equation with application to Icelandic basalts, Earth Planet. Sci. Lett. 37 (1978) 380–392.
[25] K.P. Jochum, A.W. Hofmann, E. Ito, H.M. Seufert, W.M. White, K, U, and Th in mid-ocean ridge basalt glasses and heat production, K/U, and K/Rb in the mantle, Nature 306 (1983) 431–436.
[26] H.E. Newson, W.M. White, K.P. Jochum, A.W. Hofmann, Siderophile and chalcophile element abundances in oceanic basalts. Pb isotope evolution and growth of the Earth's core, Earth Planet. Sci. Lett. 80 (1986) 299–313.
[27] K.P. Jochum, H.M. Seufert, B. Spettel, H. Palme, The solar system abundances of Nb, Ta, and Y, and the relative abundances of refractory lithophile elements in differentiated planetary bodies, Geochim. Cosmochim. Acta 50 (1986) 1173–1183.
[28] H. Bougault, J.-L. Joron, M. Treuil, Alteration, fractional crystallization, partial melting, mantle properties from trace elements in basalts recovered in the North Atlantic, in: M. Talwani, C.G. Harrison, D.E. Hayes (Eds.), Deep Drilling Results in the North Atlantic: Ocean Crust, Am. Geophys. Union, 1979, pp. 352–368.
[29] C. Dupuy, J.M. Liotard, J. Dostal, Zr/Hf fractionation in intraplate basaltic rocks: carbonate metasomatism in the mantle source, Geochim. Cosmochim. Acta 56 (1992) 2417–2423.
[30] P. Schiano, C.J. Allègre, B. Dupré, E. Lewin, J.-L. Joron, Variability of trace elements in basaltic suites, Earth Planet. Sci. Lett. 119 (1993) 37–51.
[31] G.N. Hanson, Evolution of the suboceanic mantle, J. Geol. Soc. London 134 (1977) 235–253.
[32] M.F. Thirwall, T.E. Smith, A.M. Graham, N. Theodorou, P. Hollings, J.P. Davidson, R.J. Arculus, High field strength element anomalies in arc lavas: source or process?, J. Petrol. 35 (1994) 819–838.
[33] J.P. Davidson, Deciphering mantle and crustal signatures in subduction zone magmatism, in: Bedout, Schill, Kirby (Eds.), Dynamics of Subduction, Am. Geophys. Union Geophys. Monogr. (in press).
[34] J.A. Pearce, D.W. Peate, Tectonic implications of the composition of volcanic arc magmas, Annu. Rev. Earth Planet. Sci. 23 (1995) 251–285.
[35] M. Gurnis, G.F. Davies, Mixing in numerical models of mantle convection incorporating plate kinematics, J. Geophys. Res. 91 (1986) 6375–6395.
[36] S.P. Grand, D.V. Helmburger, Upper mantle shear structure of North America, Geophys. J. R. Astron. Soc. 76 (1984) 399–438.
[37] U. Christensen, Effects of phase transformations on mantle convection, Annu. Rev. Earth Planet. Sci. 23 (1995) 65–87.